Non-linear pulsations in Wolf-Rayet stars

The non-linear evolution of strange modes

Sebastian Wende[1], Wolfgang Glatzel[1], Sonja Schuh[1]

[1]Institut für Astrophysik, Georg-August-Universität Göttingen, Friedrich-Hund-Platz 1, D–37077 Göttingen, Germany

Abstract

Numerical simulations of the evolution of strange-mode instabilities into the non-linear regime have been performed for a wide range of stellar parameters for Wolf-Rayet stars. It has been shown that the Wolf-Rayet models reach radial velocities which amount up to 30% of their escape velocity. The acoustic luminosities suggest a connection to the observed mass loss. Most of the models show a *jump* in the mean effective temperature after reaching the non-linear regime. This *jump* is related to the run of the opacity.

Non-Linear Simulations of Wolf-Rayet stars

Non-linear simulations To determine the fate of unstable stars, the evolution of their instabilities has to be followed into the non-linear regime by numerical simulations (Grott et al. 2005, MRAS, 360,1532-1544). The evolution of stellar instabilities and pulsations is followed by solving the equations of mass conservatiuon, momentum conservation, energy conservation and the diffusion equation for energy transport together with an equation of state and a prescription for the opacity.

***Strange modes* in Wolf-Rayet stars** Earlier linear stability analyses have shown that strong instabilities with high growth rates prevail in many types of massive stars. These are associated with so called *strange modes* (Gautschy & Glatzel et al. 1990, MRAS, 245,597-613). Models of Wolf-Rayet stars exhibit the strongest *strange mode* instabilities (Glatzel et al. MRAS, 262,L7-L11). Thus they are very interesting candidates for a non-linear stability analysis.

Radial velocity amplitudes The investigated Wolf-Rayet models reach final radial velocity amplitudes in the non-linear regime of the order of $10^7 cm/s$.

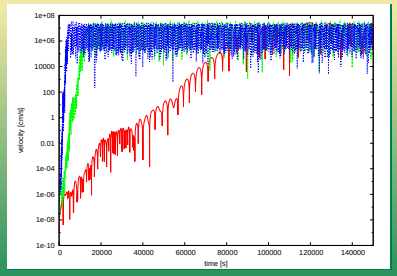

Figure 1: Modulus of the photospheric radial velocity on a logarithmic scale as a function of time for a $13.04M_\odot$ Wolf-Rayet model with different initial effective temperatures ($120.000K$ blue, $90.000K$ green and $60.000K$ red). The radial photospheric velocity evolves from the hydrostatic configuration (numerical noise) through a phase of exponential growth (linear regime) into non-linear saturation.

Acoustic Luminosities and Mass Loss Rates

Acoustic luminosities To investigate a possible connection between stellar instabilities and a pulsationally driven mass loss, the acoustic energy flux is used. It represents the mechanical energy transferred to the star's atmosphere by shock waves (Grott et al. 2005, MRAS, 360,1539). The non-linear simulation provides the time integrated acoustic luminosity as a non-monotonic function of time. We derive the mean acoustic luminosity from the mean slope of this function (see figure 2 below).

Mass loss rates With the mean acoustic luminosity it is possible to estimate a mass loss rate. We identify the mean acoustic luminosity with the "mechanical" energy of the stellar wind given by the relation $\frac{1}{2}\dot{M}v_\infty^2 = L_{acoustic}$ to determine the mass loss rate. We emphasize that the acoustic luminosity and thus the mass loss rate depends strongly on the artificial viscosity which had to be used in the simulations. Since viscosity has a dissipative effect the derived mass loss rates have to be regarded as lower limits (see table 1).

$M\ [M_\odot]$	$T_{initial}\ [K]$	$L_{acou.}\ [erg/s]$	$\dot{M}\ [M_\odot/a]$
7.021	60000	5.00E+033	1.40E-008
7.021	90000	2.55E+032	3.17E-010
9.027	60000	2.64E+034	7.50E-008
9.027	90000	1.54E+033	1.95E-009
13.040	60000	8.17E+034	2.30E-007
13.040	90000	6.78E+033	8.44E-009
17.050	60000	6.84E+034	1.87E-007
17.050	90000	1.95E+035	2.37E-007

Table 1:Acoustic luminosities and related mass loss rates for different models with different initial effective temperatures.

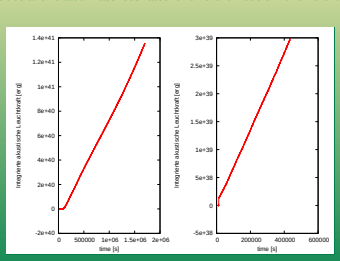

Figure 2: Time integral of the acoustic luminosity as a function of time for a $13.04M_\odot$ model with initial effective temperatures of $60.000K$ (left) and $90.000K$ (right).

Temperature *jumps*

Run of the effective temperature The *jump* of models in the mean effective temperature after reaching the non-linear regime (see figure 3) is noteworthy. All unstable models show this behaviour. The finally reached mean effective temperature is entirely independent of mass and largely independent of the initial effective temperature. There are only two final mean effective temperatures around $30.000K$ and $15.000K$ respectively. All models with an initial effective temperature above $\approx 32.000K$ jump on a mean effective temperature around $30.000K$, models with initial temperatures below this value jump on a mean effective temperature around $15.000K$.

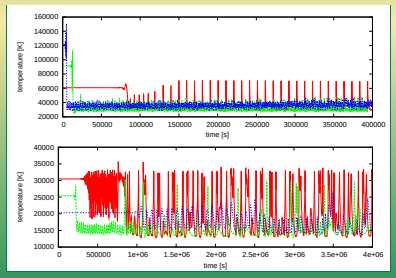

Figure 3: Effective temperature as a function of time for a $13.04M_\odot$ model with different initial effective temperatures. Top panel: Models which *jump* on a mean effective temperature around $30.000K$ from different initial effective temperatures ($120.000K$ blue, $90.000K$ green and $60.000K$ red). Bottom panel: Models which *jump* on a mean effective temperature around $15.000K$ from different initial effective temperatures ($30.000K$ blue, $25.000K$ green and $20.000K$ red).

The run of the opacity and the position of the models in the HRD

***Magic* temperatures** From the non-linear simulations we found that there are only two final mean effective temperatures for a wide range of initial effective temperatures. Considering the run of the opacity, these two temperatures correspond to the descending branches of the opacity maxima towards lower temperatures (see figure 4). Should this concept be correct, a third *magic* temperature above $\approx 100.000K$ would be expected.In fact, some models show a jump to this temperature.

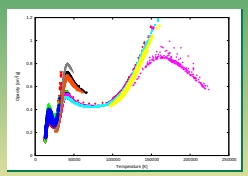

Figure 4: Run of the opacity in the stellar envelope as a function of temperature. Different stellar models were used (different colours correspond to different models), to cover a wide range of temperatures. The first maximum corresponds to the first He-Ionisation, the second maximum to the second He-Ionisation. The third maximum is caused by the contribution of heavy elements.

Final positions in the HRD The final position of the simulated models in the HRD is of particular interest. Most of the models presented move to the right and settle in a narrow temperature strip (figure 5). It is remarkably close to the obeserved positions of Wolf-Rayet stars. We emphasize that we have not yet taken into account different chemical compositions for the Wolf-Rayet models. Whether the chemical composition has a strong influence on the final mean effective temperatures remains to been seen.

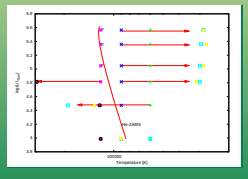

Figure 5: Hertzsprung-Russell-Diagramm of the simulated models. Indicated are the initial models with the initial effective temperatures (cruxes and stars) and the mean final effective temperatures (squares and circles). The mean luminosities stay constant. Arrows indicate the direction of the evolution. For models with question marks, we were not able to determine a final mean temperature. Models without arrows don't change their mean temperature. The He-ZAMS is shown for comparison.